Since January 2020 Elsevier has created a COVID-19 resource centre with free information in English and Mandarin on the novel coronavirus COVID-19. The COVID-19 resource centre is hosted on Elsevier Connect, the company's public news and information website.

Vaccine 40 (2022) 714–725

Contents lists available at ScienceDirect

Vaccine

journal homepage: www.elsevier.com/locate/vaccine

Intranasal immunization with a Middle East respiratory syndrome-coronavirus antigen conjugated to the M-cell targeting ligand Co4B enhances antigen-specific mucosal and systemic immunity and protects against infection

Ye Lin Yang [a,1], Ju Kim [b,1], Yongsu Jeong [c], Yong-Suk Jang [a,b,*]

[a] Department of Bioactive Material Sciences and Research Center of Bioactive Materials, Jeonbuk National University, Jeonju 54896, Korea
[b] Department of Molecular Biology and the Institute for Molecular Biology and Genetics, Jeonbuk National University, Jeonju 54896, Korea
[c] Graduate School of Biotechnology, Kyung Hee University, Yongin 17104, Korea

ARTICLE INFO

Article history:
Received 19 August 2021
Received in revised form 20 December 2021
Accepted 25 December 2021
Available online 30 December 2021

Keywords:
Adjuvant
Ligand
MERS-CoV
Recombinant antigen
Vaccine

ABSTRACT

Middle East respiratory syndrome (MERS) is a threat to public health worldwide. A vaccine against the causative agent of MERS, MERS-coronavirus (MERS-CoV), is urgently needed. We previously identified a peptide ligand, Co4B, which can enhance antigen (Ag) delivery to the nasal mucosa and promote Ag-specific mucosal and systemic immune responses following intranasal immunization. MERS-CoV infects via the respiratory route; thus, we conjugated the Co4B ligand to the MERS-CoV spike protein receptor-binding domain (S-RBD), and used this to intranasally immunize C57BL/6 and human dipeptidyl peptidase 4-transgenic (hDPP4-Tg) mice. Ag-specific mucosal immunoglobulin (Ig) A and systemic IgG, together with virus-neutralizing activities, were highly induced in mice immunized with Co4B-conjugated S-RBD (S-RBD-Co4B) compared to those immunized with unconjugated S-RBD. Ag-specific T cell-mediated immunity was also induced in the spleen and lungs of mice intranasally immunized with S-RBD-Co4B. Intranasal immunization of hDPP4-Tg mice with S-RBD-Co4B reduced immune cell infiltration into the tissues of virus-challenged mice. Finally, S-RBD-Co4B-immunized mice exhibited were better protected against infection, more likely to survive, and exhibited less body weight loss. Collectively, our results suggest that S-RBD-Co4B could be used as an intranasal vaccine candidate against MERS-CoV infection.

1. Introduction

The causative agent of Middle East respiratory syndrome (MERS) is MERS-coronavirus (MERS-CoV). MERS is a disease that significantly threatens human life. Outbreaks of MERS have occurred in the Middle East since it was first identified in 2012; however, no approved vaccine is currently available [1]. MERS-CoV is a large, positive-sense, single-strand RNA virus that consists of four structural proteins: membrane (M), envelope (E), nucleocapsid (N), and spike (S) [2–4]. The S protein forms a trimer at the virus surface and comprises S1 and S2 subunits; it plays essential roles in viral binding, membrane fusion, and host cell entry. The S1 subunit of the S protein has a receptor-binding domain (RBD), which binds to the host cell receptor protein human dipeptidyl peptidase 4 (DPP4), and less efficiently to murine DPP4 [5,6]. The S2 subunit contains two regions, heptad repeat (HR) 1 and HR2, which align to form a six-helix structure, enabling fusion of

Abbreviations: Ab, antibody; Ag, antigen; APC, allophycocyanin; CTL, cytotoxic T lymphocyte; DPP4, dipeptidyl peptidase 4; E, envelope; ELISA, enzyme-linked immunosorbent assay; ELISPOT, enzyme-linked immunosorbent spot; FBS, fetal bovine serum; FITC, fluorescein isothiocyanate; hDPP4, human DPP4; hDPP4-Tg, hDPP4-transgenic; IFN-γ, interferon-γ; Ig, immunoglobulin; IL, interleukin; M, membrane; M cell, microfold cell; MERS, Middle East respiratory syndrome; MERS-CoV, MERS-coronavirus; MERS-CoV-S, MERS-CoV spike; N, nucleocapsid; PBS, phosphate-buffered saline; PCR, polymerase chain reaction; PE, phycoerythrin; PFU, plaque-forming unit; qRT-PCR, quantitative real-time reverse-transcription PCR; RBD, receptor-binding domain; S, spike; SC, secreting cell; SE, standard error; S-RBD, RBD of the S1 subunit; Th1, T helper 1; Th2, T helper 2; TNF-α, tumor necrosis factor-α; upE, upstream E.

* Corresponding author at: Department of Molecular Biology, Jeonbuk National University, Jeonju 54896, Korea.
E-mail address: yongsuk@jbnu.ac.kr (Y.-S. Jang).
[1] These two authors contributed equally to this work.

https://doi.org/10.1016/j.vaccine.2021.12.057
0264-410X/

the virus to host cell membranes. The E and M proteins are present in the viral envelope membrane, where they are required for viral assembly, budding, and intracellular trafficking [2]. Consequently, the RBD of the S1 subunit (S-RBD) is a major target antigen (Ag) for vaccine development against MERS-CoV infection.

The nasal mucosa is an attractive route for vaccine administration due to its lack of secreted enzymes, weak acidity, and limited mucosal surface area, which typically lead to relatively low Ag dose requirements for effective vaccination [7]. Moreover, intranasal immunization induces both mucosal and systemic immune responses, as demonstrated in mice intranasally immunized against tetanus and diphtheria toxins [8], influenza virus [9], and *Streptococcus mutans* [10]. Animal studies have also revealed that potent immune responses can be induced in the genital and respiratory tracts following intranasal immunization due to activation of the common mucosal immune system [11,12]. Previously, we identified a 12-mer Co4B ligand as a targeting peptide capable of eliciting a nasal mucosal immune response; we achieved this by bio-panning a phage display library against an *in vitro* microfold cell (M cell) co-culture system [13,14]. The targeting function of Co4B to nasopharynx-associated lymphoid tissue M cells was confirmed using enhanced green fluorescence protein and *Actinobacillus pleuropneumoniae* Ag. Additionally, intranasally immunizing mice with Co4B ligand-conjugated *Actinobacillus pleuropneumoniae* Ag induces an efficient Ag-specific response in the nasal immune inductive site and lung tissue, as well as a systemic immune response capable of preventing pathogenesis following bacterial challenge [14].

In this study, we investigated the effectiveness of the Co4B ligand as an adjuvant for intranasal vaccination with the MERS-CoV Ag, S-RBD, in mice. We found that immunization with Co4B-conjugated Ag induced efficient Ag-specific systemic and mucosal immune responses in mice, and that the induction of T helper 1 (Th1) cells, cytokine responses, and Ag-specific activated T cells played important roles in protecting the mice against MERS-CoV, especially when Co4B was applied as an adjuvant. We evaluated the antiviral efficacy of Co4B-conjugated S-RBD (S-RBD-Co4B) by virally challenging mice and monitoring their weight and survival rates, and by performing histological examinations of the lung and spleen tissues of infected mice.

2. Materials and methods

2.1. Experimental materials and animals

The female C57BL/6 mice used for this experiment were purchased from Koatech Laboratory Animal Center (Pyeongtaek, Korea) and hDPP4-transgenic (hDPP4-Tg) mice were generated as previously reported [15]. The mice were maintained under specific pathogen-free conditions with food and water provided *ad libitum*. Five mice were used in each experimental group, and the experimental timeline is depicted in Fig. 1B. The animal experiments were approved by the Institutional Animal Care and Use Committee of Jeonbuk National University (Approval No. CBNU-2019–00202) and the guidelines suggested by the committee were followed. Experiments using MERS-CoV were performed in accordance with the World Health Organization's recommendations, under biosafety level 3 conditions in a biosafety level 3 facility of the Korea Zoonosis Research Institute at Jeonbuk National University (Iksan, Korea). Unless otherwise specified, the chemical and laboratory materials used in this study were obtained from Sigma Chemical Co. (St. Louis, MO, USA) and SPL Life Sciences (Pocheon, Korea), respectively.

2.2. Expression of Co4B-conjugated S-RBD Ag

The Co4B ligand (N'-HTLGFTVPTHAK-C') was conjugated to the C-terminus of the S-RBD (amino acid residues 291–725) [16] (Fig. 1A) via polymerase chain reaction (PCR). The forward primer used to amplify S-RBD and S-RBD-Co4B was 5′-GAG CTC AAG TAT TAT TCT ATC ATT CCT-3′ (*Sac*I restriction site underlined). The reverse primers used to amplify S-RBD and S-RBD-Co4B were 5′-GGA TCC TTA CTC TAC GAA CAA AGA GGA-3′ and 5′-GGA TCC TTA *CTT AGC ATG AGT AGG AAC CGT AAA ACC CAG CGT ATG* CTC TAC GAA CAA AGA GGA-3′, respectively (*Bam*HI restriction sites are underlined; Co4B peptide ligand is italicized). The amplified recombinant S-RBD and S-RBD-Co4B genes were cloned into a pCold II *Escherichia coli* expression vector system (Takara Bio, Shiga, Japan). The recombinant proteins were expressed using BL21(DE3) *E. coli* cells and purified using Ni-NTA agarose (Qiagen, Hilden, Germany). The identities of the recombinant Ags were confirmed by sodium dodecyl sulfate–polyacrylamide gel electrophoresis and Western blotting using anti-6 × His tag (Qiagen) and polyclonal anti-RBD antibodies (Abs), as described previously [17]. The protein Ags were > 95% pure. The residual endotoxin was removed by sterile filtration using Sartobind Q75 column (Sartorius, Goettinggen, Germany). The final endotoxin content was < 0.5 EU/μg of protein, as determined by the LAL chromogenic endotoxin quantitation kit (Thermo Fisher Scientific, Rockford, IL, USA).

2.3. Immunization and challenge infection of mice

C57BL/6 or hDPP4-Tg mice were immunized via the intranasal route once per week for 5 weeks, using phosphate-buffered saline (PBS) as a negative control or 10 μg of S-RBD or S-RBD-Co4B Ag (Fig. 1B). Fecal immunoglobulin (Ig) A and serum IgG were collected from the mice 3 days after the fifth immunization. Fecal samples were collected by placing each mouse in a metabolic or ordinary cage for up to 30 min, and the weight of the collected feces was measured. To prepare fecal extracts, 1 mL PBS with 0.01% sodium azide was added to 100 mg fecal samples, followed by vortexing for 10 min at room temperature. Extracts were collected by centrifugation for 10 min at 13,000 rpm at 4℃. Splenocytes and lung lymphocytes were obtained 10 days after the fifth immunization. To prepare splenocytes, mice were sacrificed and their spleens were collected. Splenocytes were collected in RPMI-1640 medium supplemented with 10% fetal bovine serum (FBS; Hyclone, Logan, UT, USA) and antibiotics after removing red blood cells by treatment with ACK lysis buffer. To prepare lung lymphocytes, the lungs were carefully obtained from the mice and then minced into small fragments using scissors. The minced tissues were digested by collagenase D, and then the lymphocytes were collected via Percoll density gradient centrifugation. Finally, after filtering the cells using a cell strainer (40 μm), the lung lymphocytes in a single cell state were prepared in RPMI-1640 medium supplemented with 10% FBS and antibiotics.

MERS-CoV was propagated in Vero E6 cells and used to assess the morbidity and mortality in hDPP4-Tg mice. The hDPP4-Tg mice were inoculated intranasally with 10^4 or 10^5 plaque-forming units (PFUs) of MERS-CoV in a total volume of 60 μL after the fifth immunization. To test the efficacy of booster, mice were immunized with their cognate Ag (S-RBD or S-RBD-Co4B) 28 days after the fifth immunization. Fecal IgA and serum IgG were collected 3 days after the boost immunization, and splenocytes and lung lymphocytes were collected 10 days after the booster.

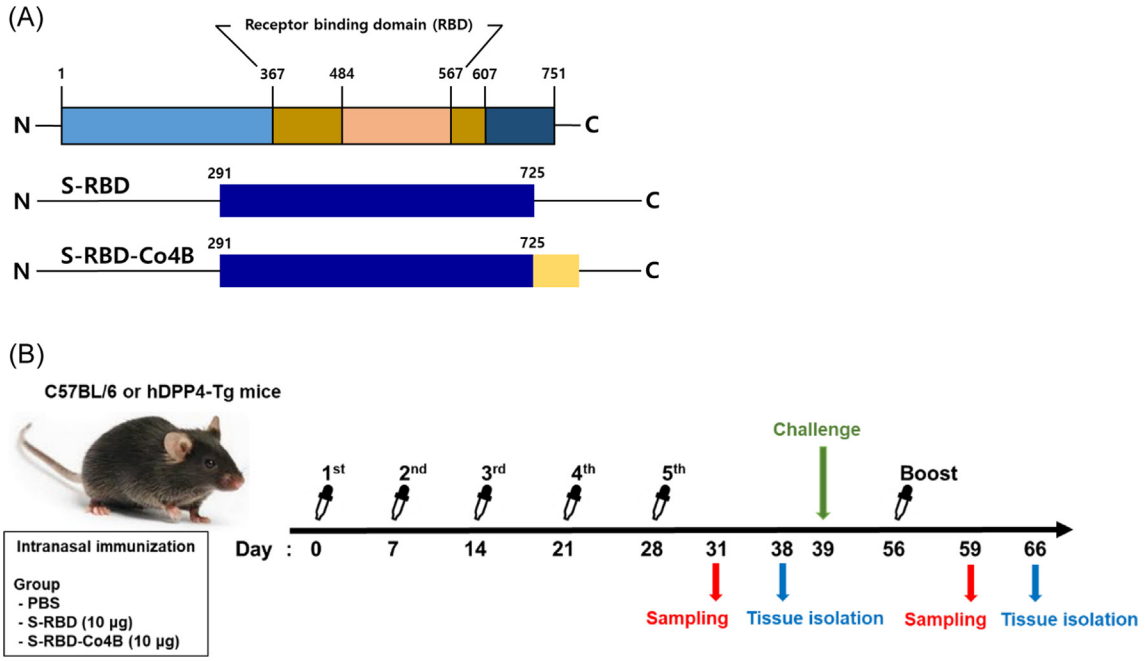

Fig. 1. Recombinant antigen (Ag) structures and the mouse immunization and experimental schedule. (A) Structural diagram of Middle East respiratory syndrome-coronavirus (MERS-CoV) receptor-binding domain (RBD) region and constructs of S-RBD and Co4B-conjugated S-RBD (S-RBD-Co4B), which were the Ags used in this study. (B) Intranasal immunization schedule for C57BL/6 and hDPP4-Tg mice immunized with phosphate-buffered saline (PBS), S-RBD, and S-RBD-Co4B. For each vaccination group, five mice were immunized at 7-day intervals (total of five times) with 10 μg of Ag. Fecal and serum samples were collected 3 days after the fifth immunization. Ten days after the fifth immunization, splenocytes and lung lymphocytes were collected from two of the five mice. Then, the remaining mice were challenged with MERS-CoV (10^4 or 10^5 plaque-forming units [PFUs]) on day 30 and booster-immunized with cognate Ags on day 56. Similarly, fecal and serum samples, and splenocytes and lung lymphocytes, were collected 3 and 10 days after the booster immunization, respectively.

2.4. Enzyme-linked immunosorbent assay (ELISA)

Ag-specific IgA and IgG from fecal and serum samples, respectively, were measured using indirect ELISAs. Briefly, 96-well ELISA plates (MaxiSorp™ immunoplate; Thermo Fisher Scientific, Roskilde, Denmark) were coated with S-RBD protein (100 ng/well) dissolved in 100 mM bicarbonate/carbonate buffer (pH 9.6) and incubated overnight at 4 °C, then blocked with 5% non-fat dry milk for 2 h at 37 °C. After adding serially diluted sample to each well, the plates were incubated for 2 h at 37 °C, then washed with PBS containing Tween 20. Then, the bound Abs were incubated with alkaline phosphatase-conjugated anti-mouse IgA or IgG secondary Ab for 2 h at 37 °C, after which *p*-nitrophenyl phosphate substrate was added. The absorbance at 405 nm was read using an ELISA plate reader (SPECTROstar Nano; BMG Labtech, Ortenberg, Germany). The Ab concentrations were calculated using a standard curve.

2.5. Ab-mediated virus inhibition assay

The Vero E6 cells used for the virus inhibition assay were cultured in Dulbecco's modified Eagle's medium (Welgene, Gyungsan, Korea) supplemented with 10% heat-inactivated FBS and 5% CO_2 at 37 °C. To measure Ag-specific Ab-mediated inhibition of the hDPP4 receptor and MERS-CoV, virus was pre-incubated with Abs collected from intranasally immunized mice for 30 min at room temperature, and then applied to Vero E6 cells (5–10 × 10^5/well).

The viral loads of MERS-CoV-infected Vero E6 cells were determined by measuring the level of upstream E (upE) gene transcript via quantitative real-time reverse-transcription PCR (qRT-PCR). Briefly, total RNA was extracted using TRI Reagent according to the manufacturer's instructions. RNA was converted into cDNA using an M−MLV Reverse Transcription Kit (Promega, Madison, WI, USA). qRT-PCR was performed using Power SYBR® Green PCR Master Mix (Thermo Fisher Scientific) and an Applied Biosystems 7500 RT-PCR system (software version 2.3; Applied Biosystems, Foster City, CA, USA). The forward and reverse primer sequences for amplifying the upE gene were 5′-GCC TCT ACA CGG GAC CCA TA-3′ and 5′-GCA ACG CGC GAT TCA GTT-3′, respectively. The forward and reverse primer sequences used to amplify the internal control gene β-actin were 5′-CGT ACC ACA GGC ATT GTG A-3′ and 5′-CTC GTT GCC AAT AGT GAT GA-3′, respectively.

2.6. Enzyme-linked immunosorbent spot assay

To measure the number of IgG-secreting cells (SCs) in splenocytes, an enzyme-linked immunosorbent spot assay (ELISPOT) assay was performed. The wells of Multi-Screen filter plates (Millipore, Billerica, MA, USA) were activated with 35% ethanol, precoated with goat anti-mouse IgG (100 ng/well; Bethyl Laboratories, Montgomery, TX, USA) and incubated overnight at 4 °C. Next, the wells were blocked with RPMI-1640 medium (Welgene) containing 10% heat-inactivated FBS, and 10^4 cells prepared from the tissues were then added to each well and incubated for 24 h at 37 °C. Horseradish peroxidase-conjugated secondary Ab was subsequently added to each well and incubated for 2 h. The membranes were then developed using 3-amino-9-ethyl-carbazole substrate solution containing 5 μL/10 mL of 30% H_2O_2. When the spots reached the desired intensity, the reaction was stopped by washing the membrane with water.

2.7. Ab-mediated virus inhibition assay using MERS-CoV spike pseudovirus

Retroviruses pseudotyped with MERS-CoV spike (MERS-CoV-S) and β-galactosidase (Lac Z) reporter genes were produced in GP2-293 cells and immediately used for the inhibition assay. Briefly, 100-fold diluted mouse immune serum samples or fecal

extracts were incubated for 1 h at room temperature with 50 μL of MERS-CoV-S pseudovirus-containing supernatants and transferred to Vero E6 cells (1.5×10^5 cells/well) grown in a 6-well tissue culture plate. After 24 h of incubation, total RNA was extracted and subjected to qRT-PCR using specific primers for β-galactosidase (5′-GGG TTG TTA CTC GCT CAC ATT-3′ and 5′-CGG TTT ATG CAG CAA CGA G-3′) and Vero E6 β-actin (5′-ATC GTG CGT GAC ATT AAG GAG-3′ and 5′-AGG AAG GAA GGC TGG AAG AG-3′) genes to measure the relative β-galactosidase gene expression mediated by MERS-CoV-S pseudovirus infection. The relative expression level of the β-galactosidase gene was normalized to the expression level of the endogenous control gene, β-actin, and calculated in terms of the fold difference using CFX Maestro software (Bio-Rad Laboratories, Hercules, CA, USA). The level in the PBS-treated sample was used as the reference (i.e., value of 1).

2.8. Abs and flow cytometry

The expression markers of lymphocytes harvested from spleen and lung tissues (performed as described previously [18]) were examined via flow cytometry. The following Abs against mouse lymphocyte expression markers were purchased from Miltenyi Biotec Inc. (Bergisch Gladbach, Germany): anti-CD3-fluorescein isothiocyanate (FITC), anti-CD4-PC5.5, anti-CD8-phycoerythrin (PE), anti-interferon-γ (IFN-γ)-allophycocyanin (APC), and anti-CD107a-APC. REA Control Ab S-FITC, REA Control Ab S-PC5.5, REA Control Ab S-PE and REA Control Ab I-APC were used as isotype controls. For intracellular staining of IFN-γ and CD107a, the lymphocytes were fixed/permeabilized using the Cytofix/Cytoperm™ Plus Fixation/Permeabilization Kit with BD GolgiStop™ protein transport inhibitor (containing monensin; BD Life Sciences, San Jose, CA, USA), according to the manufacturer's protocol. Flow cytometric analysis was performed using a Cytoflex flow cytometer (Beckman Coulter, Inc., Brea, CA, USA) and data analyses were performed using CytExpert software (Beckman Coulter, Inc.).

2.9. Measuring cytokine expression

To analyze cytokine production, harvested spleen and lung cells ($5–10 \times 10^5$) were distributed into each well of a 24-well plate and stimulated with S-RBD protein (1 μg/well) for 1 or 2 days. The culture medium was collected after stimulation and the expression levels of mouse interleukin (IL)-10, IFN-γ, and tumor necrosis factor-α (TNF-α) were quantified using a Cytometric Bead Array kit (BD Biosciences, Franklin Lakes, NJ, USA) according to the manufacturer's recommendations. Briefly, Ab-coated beads for each cytokine were mixed and incubated with the culture medium, and then incubated for 2 h at room temperature with PE-conjugated detection Abs. After washing, flow cytometric analysis was performed using a Cytoflex flow cytometer (Beckman Coulter, Inc.) and data analysis was performed using FCAP Array™ software (BD Biosciences). Cytokine concentrations were calculated using a standard curve generated using cytokine standards.

2.10. Histopathology

Spleen and lung tissue obtained from MERS-CoV- and sham-infected hDPP4-Tg mice at the time points indicated above were immediately fixed in 10% neutral-buffered formalin, transferred to 70% ethanol, and paraffin-embedded. Histopathological evaluation was performed using deparaffinized tissue sections stained with hematoxylin and eosin. We examined the MERS-CoV-infected tissues for signs of pathology, such as denatured or collapsed cell/tissue organization, hemorrhage in the interstitial space, infiltration of inflammatory monocytes, and changes in the alveolar septa.

2.11. Statistical analysis

Statistical analyses were performed using Prism 7 software (GraphPad Software Inc., San Diego, CA, USA). Results are presented as mean ± standard error (SE) of the independent replicates. Unpaired Student's *t*-tests were used to compare groups. Comparisons among groups regarding survival rate were analyzed by the log-rank test. The significance of differences between the groups was tested at $p < 0.05$, $p < 0.01$, and $p < 0.001$.

3. Results

3.1. Intranasal immunization with Co4B-conjugated S-RBD enhanced the induction of S-RBD-specific mucosal and systemic immune responses in C57BL/6 mice

We first evaluated the induction of S-RBD-specific fecal IgA and serum IgG Abs in C57BL/6 mice immunized intranasally with S-RBD or S-RBD-Co4B (Fig. 2A). The levels of S-RBD-specific fecal IgA (left) and serum IgG (right) were significantly higher ($p < 0.01$) in the mice immunized with S-RBD-Co4B compared to those immunized with S-RBD, suggesting that intranasal immunization with S-RBD-Co4B induced stronger mucosal and systemic immune responses than with unconjugated S-RBD. We next examined the ability of the S-RBD-specific Abs to prevent MERS-CoV infection in hDPP4 receptor-expressing Vero E6 cells [3] (Fig. 2B). We pre-incubated 100-fold diluted fecal samples with MERS-CoV (10^4 PFUs) and used the mixture to infect Vero E6 cells; MERS-CoV upE gene expression was significantly lower in Vero E6 cells infected with the S-RBD-Co4B-immunized mouse fecal sample compared to those infected with the PBS control samples ($p < 0.01$, 79%) and S-RBD-immunized samples ($p < 0.05$) (Fig. 2B, left). Serum samples from S-RBD-Co4B-immunized mice also inhibited upE gene expression to a significantly greater extent compared to PBS control ($p < 0.001$) and S-RBD-immunized ($p < 0.01$) mouse serum samples (Fig. 2B, right). These results indicate that Abs induced by intranasal immunization of S-RBD-Co4B effectively prevented MERS-CoV infection, possibly by inhibiting interactions between the virus and its cognate receptor.

Greater S-RBD-specific mucosal and systemic immune responses were also detected in fecal and serum samples collected 3 days after a booster immunization, 28 days after the fifth immunization, from mice immunized with S-RBD-Co4B compared to those immunized with unconjugated S-RBD (Fig. 2C). The levels of S-RBD-specific fecal IgA and serum IgG were higher in S-RBD-Co4B-immunized mice compared to mice immunized with unconjugated S-RBD. We also found a significantly higher number of S-RBD-specific IgG-secreting splenocytes in S-RBD-Co4B-immunized mice compared to S-RBD-immunized mice ($p < 0.01$; Fig. 2D). In addition, we performed the virus inhibition assay in Vero E6 cells with a MERS-CoV-S pseudovirus to confirm the neutralizing activity of the serum samples and fecal extracts prepared from booster-immunized mice (Fig. S1). We measured the transcription level of the β-galactosidase gene in Vero E6 cells infected with MERS-CoV-S pseudovirus, which had been pre-incubated with serum samples or fecal extracts via qRT-PCR. The fecal extracts (left) and serum samples (right) prepared from S-RBD-Co4B-immunized mice showed significantly ($p < 0.01$ and 0.05, respectively) higher inhibition of the β-galactosidase gene expression compared to mice immunized with either PBS or S-RBD alone. Collectively, these results suggest that S-RBD-specific mucosal IgA and systemic IgG responses were more efficiently induced in mice intranasally immunized with S-RBD-Co4B compared to unconjugated S-RBD, leading to more effective inhibition of MERS-CoV infection.

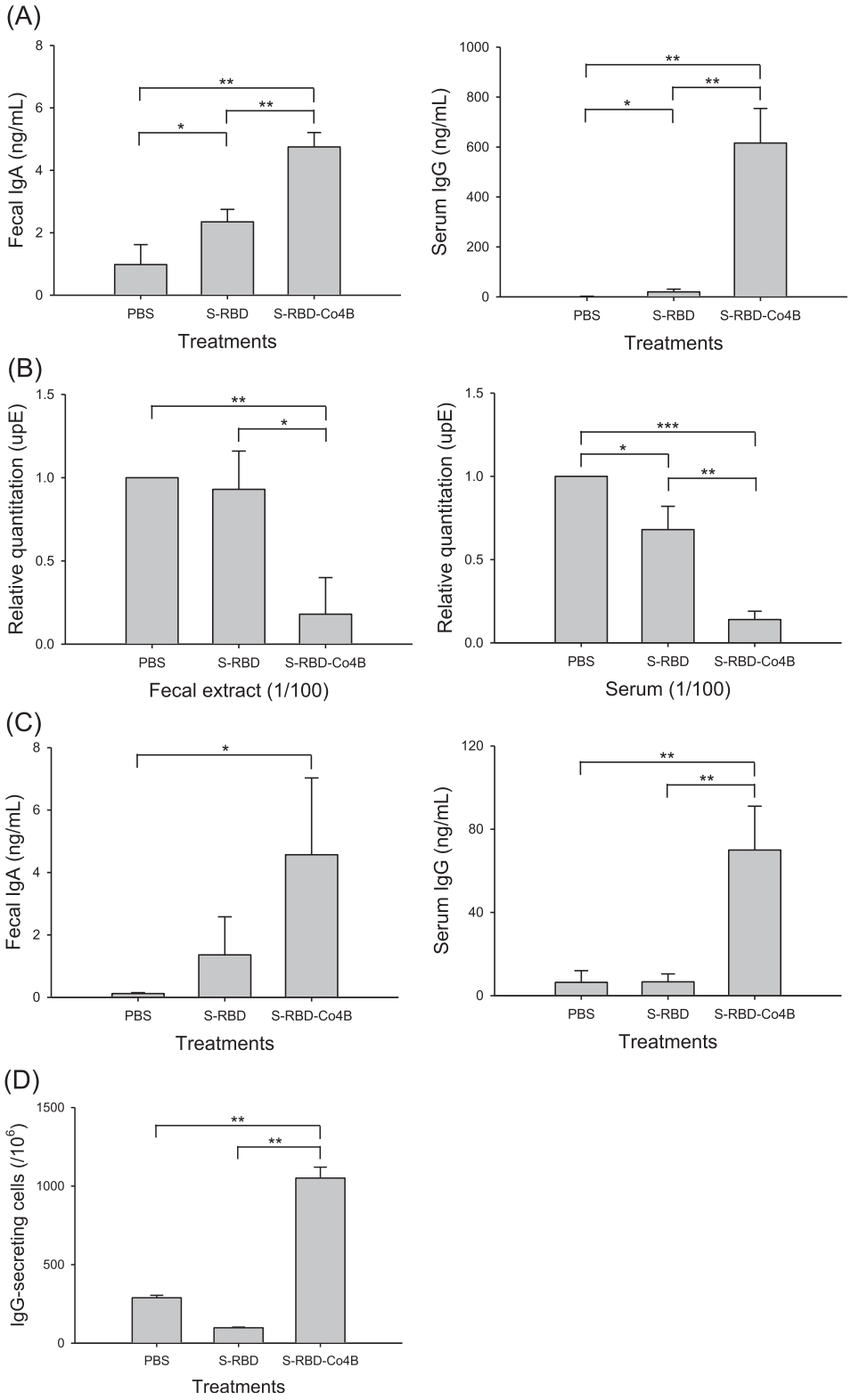

Fig. 2. Intranasal immunization with S-RBD-Co4B induces S-RBD-specific mucosal and systemic antibody (Ab) responses, together with Ab-mediated virus inhibition, in C57BL/6 mice. (A) Concentrations of fecal immunoglobulin (Ig) A (left) and serum IgG (right) in samples collected from C57BL/6 mice 3 days after the fifth immunization with indicated Ags, as determined by enzyme linked immunosorbent assay (ELISA). (B) Fecal and serum samples were pre-incubated with MERS-CoV (10^4 PFUs). Ab-mediated inhibition of MERS-CoV infection in Vero E6 cells was determined by measuring upstream E (upE) gene expression levels relative to β-actin (internal control) gene expression levels via quantitative real-time polymerase chain reaction (qRT-PCR). Data are expressed as relative quantitation with the level of PBS set as 1. (C) Concentrations of fecal IgA (left) and serum IgG (right) in samples collected from C57BL/6 mice 3 days after booster immunization with indicated Ags, as determined by ELISA. (D) Splenocytes were stimulated with 1 μg of S-RBD Ag, and the number of S-RBD-specific IgG-secreting cells per 10^4 splenocytes was determined by enzyme-linked immunosorbent spot assay. The experiments were repeated three times and representative results are presented. $^*p < 0.05$, $^{**}p < 0.01$, and $^{***}p < 0.001$.

3.2. Intranasal immunization with S-RBD-Co4B enhanced the stimulation of S-RBD-specific effector cytotoxic T lymphocytes (CTLs) in mucosal and systemic immune compartments of C57BL/6 mice

CTLs are the major cells involved in the removal of coronavirus infections, such as mouse hepatitis virus [19,20]. They are characterized by the production of Th1 cytokines, such as IFN-γ, and the expression of CD107a degranulation marker [21]. In addition, $CD4^+$ CTLs that secrete IFN-γ only, or IFN-γ with TNF-α and IL-2, can secrete cytotoxic granules containing granzyme B and kill target cells in an Ag-specific manner upon direct contact [22–24]. To assess the induction of CTL activity by intranasal immunization with Ags, splenocytes and lung lymphocytes collected from immunized mice were stimulated with S-RBD, and their expression of cell surface markers and cytokines were analyzed (Fig. 3). After 17 h of S-RBD stimulation, the frequency of IFN-γ-producing $CD4^+$ and $CD8^+$ CTLs was significantly higher in the splenocyte pool of mice immunized with S-RBD-Co4B compared to those immunized with unconjugated S-RBD ($p < 0.05$; Fig. 3A). The cytotoxic potential was relatively high in splenocytes collected from S-RBD-Co4B-immunized mice, as shown by the high intracellular expression levels of CD107a (Fig. 3B). Furthermore, effector $CD4^+$ and $CD8^+$ CTL stimulation was significantly higher in lung lymphocytes collected from mice immunized with S-RBD-Co4B compared to those immunized with unconjugated S-RBD ($p < 0.01$) (Fig. 3C). Likewise, the cytotoxic potential was significantly higher in both $CD4^+$ and $CD8^+$ lung lymphocytes harvested from mice immunized with S-RBD-Co4B compared to unconjugated S-RBD ($p < 0.05$) (Fig. 3D).

Next, we characterized the effects of intranasal immunization with Co4B-conjugated Ag on immune stimulation, by analyzing Th1 cytokine expression in splenocytes and lung lymphocytes that had been stimulated for 48 h with S-RBD (Fig. 3E). The expression levels of IL-10, IFN-γ, and TNF-α were remarkably enhanced in both splenocytes and lung lymphocytes harvested from S-RBD-Co4B-immunized mice compared to mice immunized with unconjugated S-RBD. In particular, IFN-γ expression in splenocytes and lung lymphocytes following S-RBD stimulation was greatly enhanced in S-RBD-Co4B-immunized mice. Collectively, these results suggest that intranasal immunization with Co4B-conjugated Ag efficiently induces Th1-type immune stimulation, promoting $CD4^+$ and $CD8^+$ effector CTL activity.

3.3. The Co4B ligand enhances mucosal and systemic immune responses in hDPP4-Tg mice

Next, we examined the effects of intranasal immunization with S-RBD-Co4B on the induction of S-RBD-specific mucosal and systemic immune responses in hDPP4-Tg mice, because mice expressing murine DPP4 only are not susceptible to MERS-CoV infection [25]. We evaluated the induction of S-RBD-specific fecal IgA and serum IgG in hDPP4-Tg mice that were intranasally immunized with S-RBD or S-RBD-Co4B (Fig. 4A). The levels of S-RBD-specific fecal IgA (left) and serum IgG (right) were higher in mice immunized with S-RBD-Co4B compared to S-RBD, and the difference was statistically significant for the serum samples. This suggests that intranasal immunization with S-RBD-Co4B induces higher mucosal and systemic immune responses than immunization with unconjugated S-RBD. Then, we confirmed that the Abs could inhibit MERS-CoV infections in hDPP4 receptor-expressing Vero E6 cells (Fig. 4B). We pre-incubated 100-fold diluted fecal samples with MERS-CoV (10^4 PFUs) and used the samples to infect Vero E6 cells; MERS-CoV upE gene expression was significantly lower in Vero E6 cells infected with fecal samples collected from S-RBD-Co4B-immunized mice compared to those immunized with PBS ($p < 0.01$) and unconjugated S-RBD ($p < 0.05$) (Fig. 4B, left). Serum samples collected from S-RBD-Co4B-immunized mice also exhibited significantly stronger upE gene expression inhibition compared to those collected from the PBS control ($p < 0.01$) and S-RBD-immunized mice ($p < 0.05$; Fig. 4B, right). These results indicate that Abs induced by intranasal immunization with S-RBD-Co4B efficiently inhibited MERS-CoV infection in hDPP4-Tg mice.

Next, we analyzed Th1 cytokine expression in splenocytes and lung lymphocytes that had been collected from mice intranasally immunized with Co4B-conjugated Ag, and then stimulated with S-RBD for 48 h (Fig. 4C). Similar to the results from the experiments with C57BL/6 mice, the expression of IL-10, IFN-γ, and TNF-α was significantly higher in both splenocytes ($p < 0.05$) and lung lymphocytes ($p < 0.001$) collected hDPP4-Tg mice immunized with from S-RBD-Co4B compared to unconjugated S-RBD-immunized hDPP4-Tg mice. Taken together, these results suggest that intranasal immunization with Co4B-conjugated Ag efficiently induced Th1-type immune stimulation capable of promoting $CD4^+$ and $CD8^+$ effector CTL activity in both C57BL/6 and hDPP4-Tg mice.

3.4. Intranasal immunization with S-RBD-Co4B elicits potent protective immunity and prevents lung damage in hDPP4-Tg mice challenged with MERS-CoV

In our previous study, we found that hDPP4-Tg mice challenged with 10^4 or 10^5 PFUs MERS-CoV exhibited body weight loss and mortality of 60% and 100% at 12 days post infection, respectively [15]. To determine whether intranasal immunization with S-RBD-Co4B could effectively protect hDPP4-Tg mice challenged with MERS-CoV, we monitored the body weight, survival, and tissue damage of the mice following intranasal challenge infection with MERS-CoV (Fig. 5). Following inoculation of hDPP4-Tg mice with 10^4 PFUs of MERS-CoV, there was no significant difference in body weight between the mice immunized with conjugated and unconjugated Ags (Fig. 5A, left); however, the survival rate was significantly higher in hDPP4-Tg mice immunized with S-RBD-Co4B compared to the control at 14 days after challenge infection ($p < 0.05$) (Fig. 5A, right). This protective effect was more prominent following infection with 10^5 PFUs of MERS-CoV (Fig. 5B). Body weight loss and death began to occur at 6 days after the challenge infection with 10^5 PFUs of MERS-CoV (Fig. 5B, left); the survival rate was significantly higher in mice immunized with S-RBD-Co4B (40%) compared to those immunized with PBS control and unconjugated S-RBD ($p < 0.05$; Fig. 5B, right).

We collected mouse lung and spleen tissues from the mice 7 days after MERS-CoV infection for histological analysis. We found no prominent differences in the histology of the liver, brain, or small intestine among the immunization groups (data not shown). However, the dissected lung and spleen tissues collected from hDPP4-Tg mice immunized with PBS and challenged with MERS-CoV (10^5 PFUs) exhibited marked histopathologic changes, such as inflammatory immune cell infiltration (arrows), local bronchial wall thickening, and severe lung tissue damage due to airspace expansion (arrow heads) (Fig. 5C). Although the lungs of all mice challenged with MERS-CoV displayed squamous metaplasia and epithelial hypertrophy, S-RBD-Co4B-immunized mice exhibited reduced lung tissue lesion formation compared to PBS- and S-RBD-immunized mice (Fig. 5C, upper panels). White pulp thickening, as well as marginal zone and red pulp border collapse, were observed in the spleens of MERS-CoV-challenged mice, while marginal zone expansion and white pulp widening were detected in the spleens of S-RBD-Co4B-immunized mice. Moreover, the red pulp and marginal zone borders were clearly identifiable in the spleens of S-RBD-Co4B-immunized mice (Fig. 5C, lower panels). These results suggest that intranasally immunizing hDPP4-Tg mice with S-RBD-Co4B protected lung and spleen tissues against damage due to MERS-CoV infection.

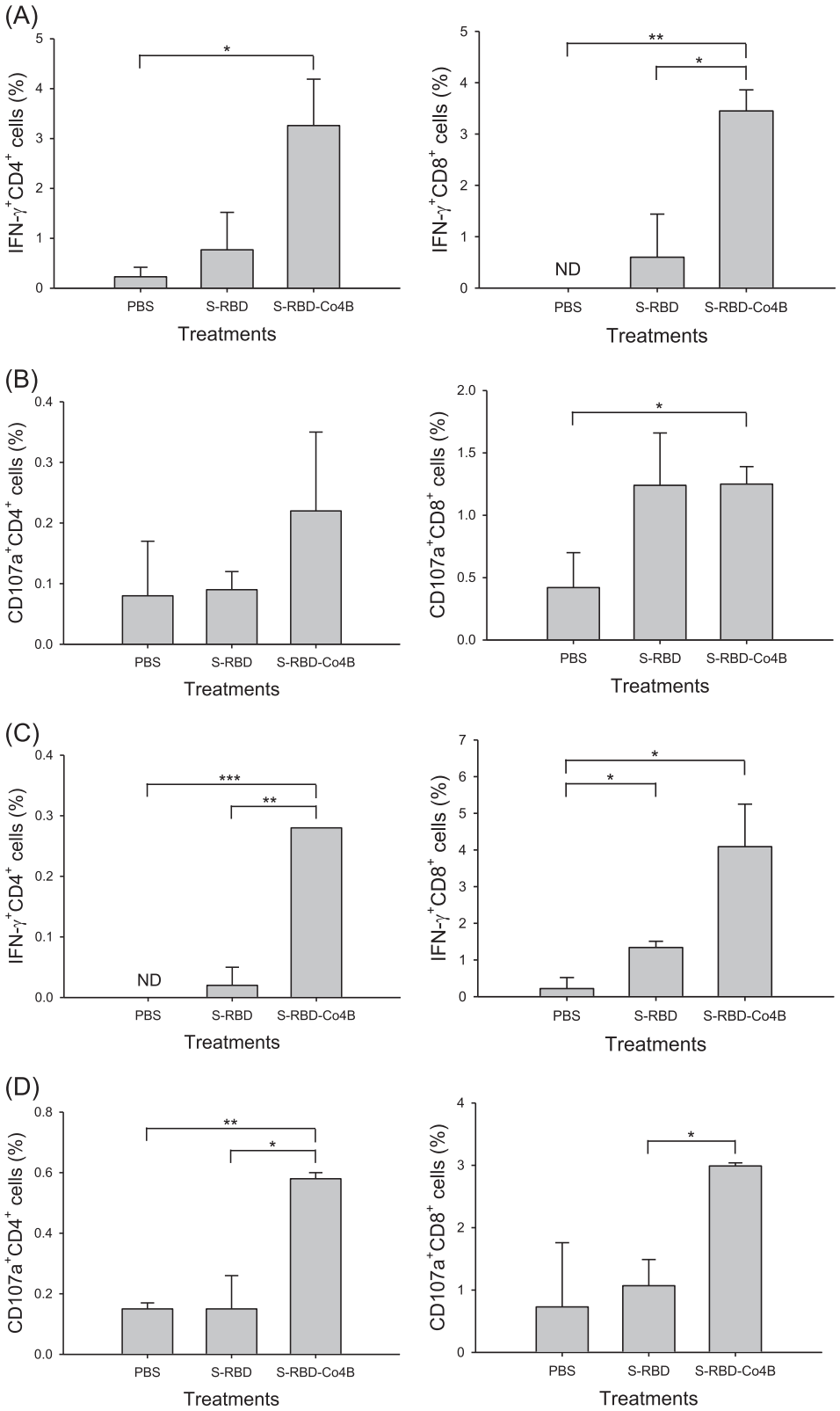

Fig. 3. Intranasal immunization with S-RBD-Co4B enhanced S-RBD-specific effector cytotoxic T lymphocyte (CTL) stimulation in splenocytes and lung lymphocytes in C57BL/6 mice. Splenocytes and lung lymphocytes were collected 10 days after the fifth immunization with the indicated Ag, and then stimulated with S-RBD (1 μg) for up to 48 h. (A) The expression of IFN-γ in $CD4^+$ (left) and $CD8^+$ (right) cells in splenocytes after stimulation with S-RBD for 17 h was analyzed by flow cytometry. (B) Expression of CD107a in $CD4^+$ (left) and $CD8^+$ (right) cells in splenocytes after stimulation with S-RBD for 24 h was analyzed by flow cytometry. (C) Expression of IFN-γ in $CD4^+$ (left) and $CD8^+$ (right) cells in lung lymphocytes after stimulation with S-RBD for 17 h was analyzed by flow cytometry. (D) Expression of CD107a in $CD4^+$ (left) and $CD8^+$ (right) cells in lung lymphocytes after stimulation with S-RBD for 24 h was analyzed by flow cytometry. (E) Cytokine concentrations in the culture supernatants collected from splenocytes (left panels) and lung lymphocytes (right panels) that had been stimulated with S-RBD (1 μg) for 48 h, as determined by cytometric bead array. Experiments were repeated three times and representative results are presented. $^*p < 0.05$, $^{**}p < 0.01$, and $^{***}p < 0.001$.

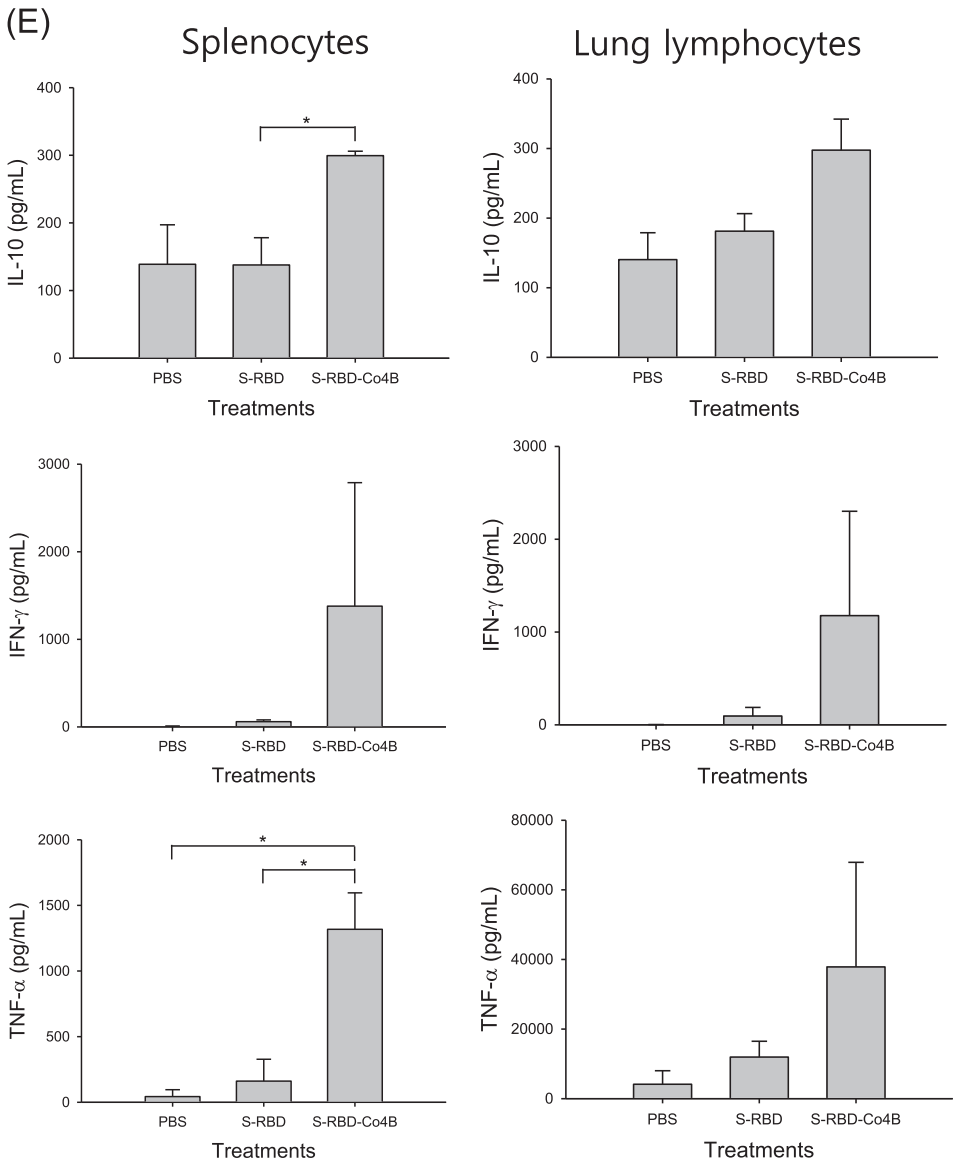

Fig. 3 (*continued*)

4. Discussion

Several MERS-CoV outbreaks have occurred since the first one in Saudi Arabia in 2012. It is crucial to develop prophylactic measures for MERS-CoV infection; in this respect, vaccines play an important role. Four types of MERS-CoV vaccines are currently being developed: inactivated virus, live-attenuated, DNA, and recombinant vaccines. However, no vaccine for MERS-CoV has been licensed to date [26]. Regarding the recombinant vaccine, various S-RBD fragments have been considered for use as the main target Ags, including amino acid residues 358–588, 367–588, 377–588, and 367–606 [27–29]. The fragment of the MERS-CoV S-RBD containing residues 377–588 is a critical neutralizing domain; it induces the strongest humoral immune response with neutralizing Abs in immunized animals, especially when fused with Fc region of human IgG [16]. Vaccination of BALB/c mice with the S-RBD residues 377–588 fused with Fc and the adjuvant MF59 elicited strong humoral and cellular immune responses at low doses [30]. Interestingly, intranasal administration of MERS-CoV S-RBD led to a more powerful local mucosal immune response in the lung tissue compared to subcutaneous immunization [27]. MERS-CoV infects the lower respiratory tract, leading to severe pneumonia and occasionally digestive symptoms such as diarrhea and nausea/vomiting; thus, mucosal membranes appear to be appropriate targets for vaccination against MERS-CoV infection [2,31]. We therefore aimed to develop a vaccine candidate using S-RBD (291–725) conjugated to the Co4B ligand, which was identified as a strong inducer of immune responses against conjugated Ags after intranasal administration (Fig. 1) [14].

The role of mucosal immunity in the lungs has not been widely studied, despite the respiratory mucosa being the main site of infection for numerous pathogens, including MERS-CoV. Intranasal immunization confers greater protective immunity against MERS-CoV infection compared to intramuscular immunization in hDPP4-Tg mice, so the development of an intranasal vaccine against MERS-CoV infection is important [15]. Typically, vaccinations contain specific Ags, and an adjuvant, to increase the immunogenicity of the Ags and their ability to induce specific adaptive immunity [32]. Here, we confirmed the adjuvant effect of the Co4B ligand on the induction of antiviral and Ag-specific immune responses to the recombinant Ag of MERS-CoV. The 12-mer Co4B ligand was previously identified by bio-panning a phage display library

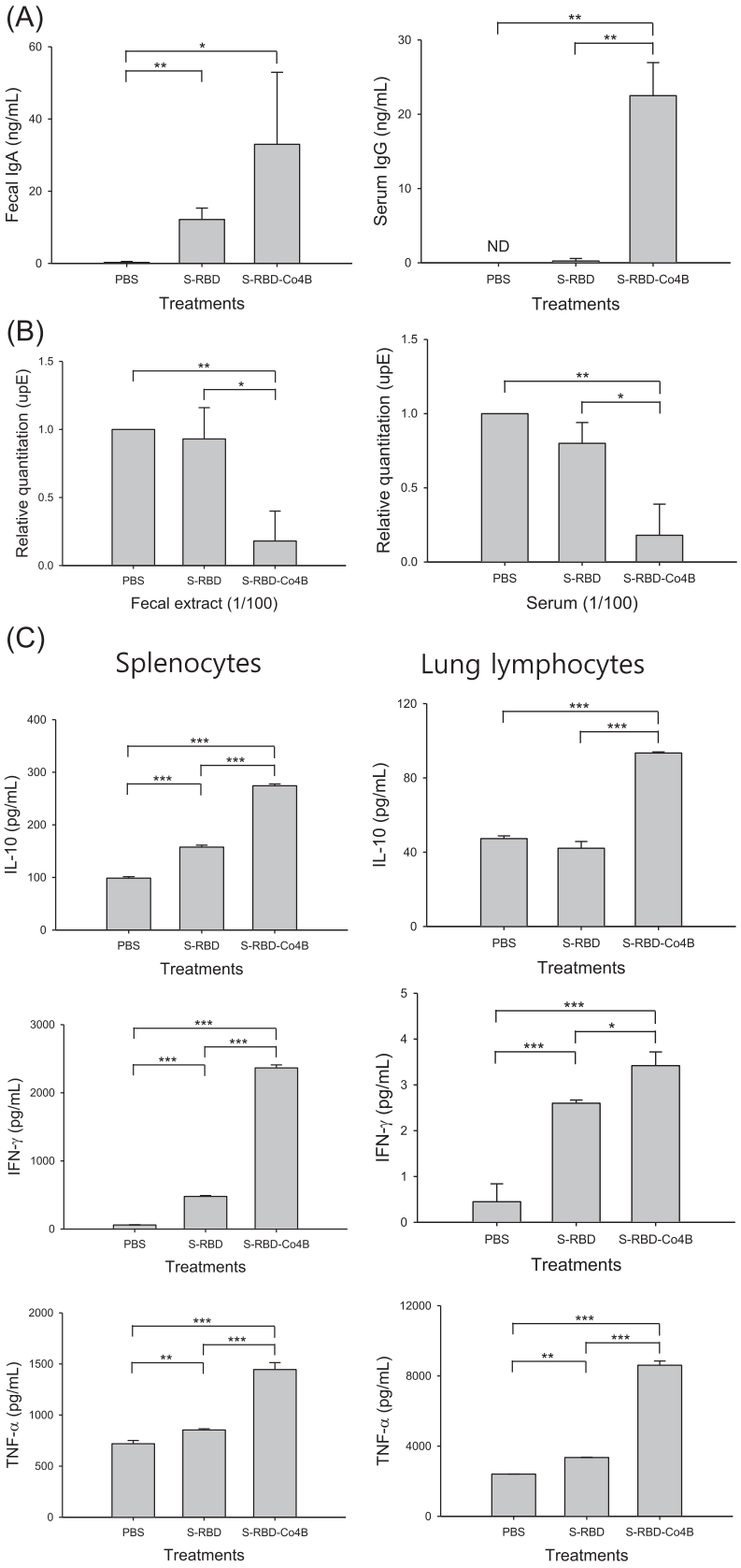

Fig. 4. Intranasal immunization with S-RBD-Co4B induces S-RBD-specific mucosal and systemic Ab responses, together with Ab-mediated virus inhibition, in hDPP4-Tg mice. (A) Concentrations of fecal IgA (left) and serum IgG (right) in samples collected from hDPP4-Tg mice 3 days after the fifth immunization with the indicated Ag, as determined by ELISA. (B) Fecal and serum samples were pre-incubated with MERS-CoV (10^4 PFUs), and Ab-mediated inhibition of MERS-CoV infection in Vero E6 cells was determined by measuring the level of upE gene expression via qRT-PCR. UpE gene expression levels were compared to those of the internal control β-actin to calculate the relative expression. Data are expressed as relative quantitation with the level of PBS set as 1. (C) Cytokine concentrations in culture supernatants collected from splenocytes (left panels) and lung lymphocytes (right panels) following stimulation with S-RBD (1 μg) for 48 h, as determined by cytometric bead array. Experiments were repeated three times and representative results are presented. $^{*}p < 0.05$, $^{**}p < 0.01$, and $^{***}p < 0.001$.

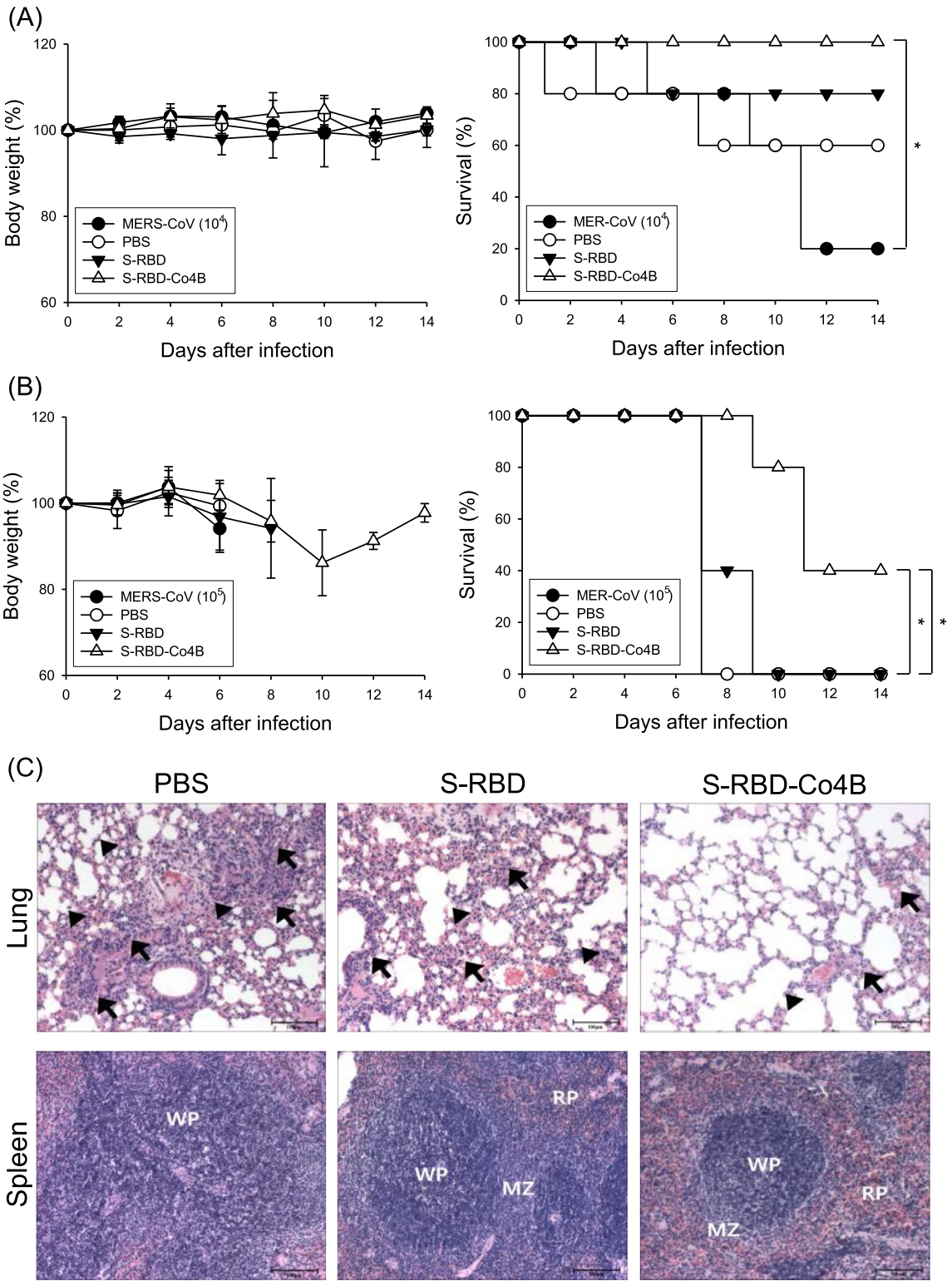

Fig. 5. Intranasal immunization with Co4B-conjugated S-RBD elicits potent protective immunity and prevents lung and spleen damage in hDPP4-Tg mice following MERS-CoV challenge infection. Mice were intranasally immunized with the indicated Ags and challenged intranasally with (A) 10^4 or (B) 10^5 PFUs of MERS-CoV. Body weight changes (left panels) and survival rates (right panels) of the mice (n = 5) were monitored every 2 days for 2 weeks. (C) Histological changes in the lung and spleen tissues of hDPP4-Tg mice immunized with indicated Ags (10 μg) and challenged with MERS-CoV (10^5 PFUs). Tissues were prepared 7 days after the challenge infection. Arrows indicate inflammatory immune cell infiltration, and arrow heads indicate airspace. RP, red pulp; WP, white pulp; MZ, marginal zone. Scale bars = 100 μm. *$p < 0.05$. (For interpretation of the references to colour in this figure legend, the reader is referred to the web version of this article.)

against an *in vitro* M−like cell culture system, and its ability to target conjugated Ags to nasal-associated lymphoid tissue M cells, to induce Ag-specific immune responses, has been demonstrated [13,14]. We also confirmed that S-RBD-Co4B can bind to nasopharynx-associated lymphoid tissue M cells (data not shown). Mucosal IgA in the respiratory tissue, together with systemic IgG,

plays important roles in host defense against respiratory virus infection [33]. Therefore, we examined the ability of Co4B to act as an adjuvant, to induce mucosal and systemic immune responses specific to MERS-CoV S-RBD, in C57BL/6 and hDPP4-Tg mice (Fig. 2A and Fig. 4A). Additionally, we confirmed that the mucosal and systemic Abs induced by S-RBD-Co4B inhibited the interaction of MERS-CoV with DPP4 to a greater extent than unconjugated S-RBD in both C57BL/6 and hDPP4-Tg mice (Fig. 2B and Fig. 4B).

Similar to cytotoxic $CD8^+$ T cells, functional $CD4^+$ T cells have cytolytic characteristics and exert protective effect against influenza virus infection [34]. Effector cells that produce IFN-γ in the lung also play a protective role at the site of infection [35]. The frequency of IFN-γ- and CD107a-expressing $CD4^+$ and $CD8^+$ T cells in splenocytes and lung lymphocytes collected from S-RBD-Co4B-immunized mice was higher than in those harvested from S-RBD-immunized mice, which suggests that Ag-specific effector CTL cells were stimulated by intranasal immunization with S-RBD-Co4B (Fig. 3). In addition, the efficient stimulation of Th1-type cytokines such as IL-10, IFN-γ, and TNF-α implies that effective cell-mediated immunity was induced by intranasal immunization with S-RBD-Co4B in both C57BL/6 and hDPP4-Tg mice (Fig. 3E and Fig. 4C). Notably, IFN-γ, which is a type II IFN, plays essential roles in controlling various viral infections and promoting viral clearance by adaptive immune cells [26]. The induction of pro-inflammatory cytokines and other IFNs is delayed following MERS-CoV infection, which has adverse effects on the host [36]. Therefore, efficient induction of IFN-γ by intranasal immunization with S-RBD-Co4B may be critical for protective immunity in MERS-CoV infection.

In previous studies, vaccine development against MERS-CoV and severe acute respiratory syndrome coronavirus has raised concerns regarding pulmonary immunopathology due to the aberrant levels of the T helper 2 (Th2) response, as vaccination of inactivated MERS-CoV into a mouse model showed an enhanced Th2 response compared to that before vaccination, as well as immunopathologic responses [37,38]. Although further research is needed to confirm the correlation, the immunopathologic response might be partly attributed to vaccination [39]. In addition to the level of Th1 responses (Fig. 3E and Fig. 4C), we also confirmed that Th2 and Th17 responses were higher in S-RBD-Co4B-immunized mice compared to mice immunized with PBS (data not shown). Many studies using murine vaccine models have shown that Th17-mediated protective responses involve IL-17-driven Th1 immune response [40]. The roles of Th17 cells have been documented in regulating B-cell Ab generation, formation of the germinal center, and inducible bronchus-associated lymphoid tissue. Therefore, mucosal vaccination can induce robust Th17 responses, which are considered useful targets for mucosal vaccination. However, Th17-mediated inflammatory responses have also been shown to be responsible for the immunopathology seen in the pathogenesis of COVID-19 pneumonia and edema [41]. These Th17 responses include the release of cytokines, including IL-17 and granulocyte–macrophage colony-stimulating factor, downregulating regulatory T cells, and promoting neutrophil recruitment, but simultaneously inducing Th2 immune responses. However, our observation of the increase in IgG2a/IgG1 in the sera of immunized mice (Fig. S2). along with the level of Th1 responses (Fig. 3E and Fig. 4C) suggest that Th1 responses are dominant in S-RBD-Co4B-immunized mice.

The hDPP4 receptor, which is recognized and used for entry by MERS-CoV, is not present in the tissues of mice, meaning that they are not susceptible to MERS-CoV infection; this has hampered MERS-CoV research. Moreover, respiratory infection and pathological lung damage are key features of severe human disease caused by MERS-CoV infection. Therefore, a transgenic animal model with consistent hDPP4 expression and pulmonary pathology is needed. Previously, we generated hDPP4-Tg mice that express hDPP4 at high levels, which enabled MERS-CoV to develop (reflected in significantly higher viral RNA levels in the brain, lung, liver, spleen, and intestinal tissues) [15]. MERS-CoV infection in the respiratory tract causes fibrotic lung disease symptoms including alveolar cell damage, inflammation, fibroblast proliferation, and extracellular matrix deposition [5]. In the present study, we detected histopathologic changes in the lung (*e.g.*, pulmonary fibrosis), which is the initial infection site, and in the spleen, a representative tissue of systemic immunity, after MERS-CoV infection in hDPP4-Tg mice (Fig. 5C). Importantly, intranasal immunization with S-RBD-Co4B prevented histopathological changes in the lung and spleen, thus confirming the efficacy of the vaccine histologically (Fig. 5C). Moreover, mice immunized intranasally with S-RBD-Co4B showed superior survival rates following infection with MERS-CoV compared to the other groups (Fig. 5A and Fig. 5B). Collectively, our findings demonstrate that S-RBD-Co4B is a promising candidate for an intranasal recombinant vaccine against MERS-CoV infection, which is capable of inducing efficient humoral and cell-mediated immunity.

Declaration of Competing Interest

The authors declare that they have no known competing financial interests or personal relationships that could have appeared to influence the work reported in this paper.

Acknowledgments

This work was supported by grants from the Basic Science Research Program (2019R1A2C2004711) and the Strategic International Collaborative Research Program (2020K1A4A7A02095058) through the National Research Foundation, which was funded by the Korean Ministry of Science and ICT. Dr. Yong-Suk Jang was supported by the Research Base Construction Fund Program funded by Jeonbuk National University in 2021. Y. L. Yang was supported by the BK21 FOUR program in the Department of Bioactive Material Sciences. Some experiments were performed using instruments installed in the Center for University-Wide Research Facilities (CURF) at Jeonbuk National University.

Authors Contributions

YLY, JK and Y-SJ designed the research; YLY, JK and YJ performed the research; YLY, JK, YJ, and Y-SJ analyzed the data; YLY, JK and Y-SJ wrote the paper; Y-SJ acquired funding and supervised the research. All authors have read and approved the final manuscript.

Appendix A. Supplementary data

Supplementary data to this article can be found online at https://doi.org/10.1016/j.vaccine.2021.12.057.

References

[1] Zumla A, Hui DS, Perlman S. Middle East respiratory syndrome. The Lancet 2015;386(9997):995–1007. https://doi.org/10.1016/S0140-6736(15)60454-8.
[2] Memish ZA, Perlman S, Van Kerkhove MD, Zumla A. Middle East respiratory syndrome. The Lancet 2020;395(10229):1063–77. https://doi.org/10.1016/S0140-6736(19)33221-0.
[3] Raj VS, Mou H, Smits SL, Dekkers DHW, Müller MA, Dijkman R, et al. Dipeptidyl peptidase 4 is a functional receptor for the emerging human coronavirus-EMC. Nature 2013;495(7440):251–4. https://doi.org/10.1038/nature12005.
[4] Walls AC, Tortorici MA, Bosch B-J, Frenz B, Rottier PJM, DiMaio F, et al. Cryo-electron microscopy structure of a coronavirus spike glycoprotein trimer. Nature 2016;531(7592):114–7. https://doi.org/10.1038/nature16988.

[5] Barlan A, Zhao J, Sarkar MK, Li K, McCray PB, Perlman S, et al. Receptor variation and susceptibility to Middle East respiratory syndrome coronavirus infection. J Virol 2014;88(9):4953–61. https://doi.org/10.1128/JVI.00161-14.

[6] van Doremalen N, Miazgowicz KL, Milne-Price S, Bushmaker T, Robertson S, Scott D, et al. Host species restriction of Middle East respiratory syndrome coronavirus through its receptor, dipeptidyl peptidase 4. J Virol 2014;88 (16):9220–32. https://doi.org/10.1128/JVI.00676-14.

[7] Ramvikas M, Arumugam M, Chakrabarti S, Jaganathan K. Nasal vaccine delivery. Micro and Nanotechnology in Vaccine Development. Elsevier 2017:279–301. https://doi.org/10.1016/B978-0-323-39981-4.00015-4.

[8] Alpar HO, Eyles JE, Williamson ED, Somavarapu S. Intranasal vaccination against plague, tetanus and diphtheria. Adv Drug Deliv Rev 2001;51(1-3):173–201. https://doi.org/10.1016/S0169-409X(01)00166-1.

[9] Fiore AE, Shay DK, Broder K, Iskander JK, Uyeki TM, Mootrey G, et al. Prevention and control of seasonal influenza with vaccines: recommendations of the Advisory Committee on Immunization Practices (ACIP), 2009. MMWR Recomm Rep 2009;58:1–52. , https://www.jstor.org/stable/24842373?seq=1#metadata_info_tab_contents.

[10] Childers NK, Li F, Dasanayake AP, Li Y, Kirk K, Michalek SM. Immune response in humans to a nasal boost with *Streptococcus mutans* antigens. Oral Microbiol Immunol 2006;21(5):309–13. https://doi.org/10.1111/j.1399-302X.2006.00302.x.

[11] Mestecky J, Raska M, Novak J, Alexander RC, Moldoveanu Z. Antibody-mediated protection and the mucosal immune system of the genital tract: relevance to vaccine design. J Reprod Immunol 2010;85(1):81–5. https://doi.org/10.1016/j.jri.2010.02.003.

[12] Brandtzaeg P. Potential of nasopharynx-associated lymphoid tissue for vaccine responses in the airways. Am J Respir Crit Care Med 2011;183(12):1595–604. https://doi.org/10.1164/rccm.201011-1783OC.

[13] Kim S-H, Seo K-W, Kim Ju, Lee K-Y, Jang Y-S. The M cell-targeting ligand promotes antigen delivery and induces antigen-specific immune responses in mucosal vaccination. J Immunol 2010;185(10):5787–95. https://doi.org/10.4049/jimmunol.0903184.

[14] Park J, Seo K-W, Kim S-H, Lee H-Y, Kim B, Lim CW, et al. Nasal immunization with M cell-targeting ligand-conjugated ApxIIA toxin fragment induces protective immunity against *Actinobacillus pleuropneumoniae* infection in a murine model. Vet Microbiol 2015;177(1-2):142–53. https://doi.org/10.1016/j.vetmic.2015.03.005.

[15] Kim Ju, Yang YL, Jeong Y, Jang Y-S. Middle East respiratory syndrome-coronavirus infection into established hDPP4-transgenic mice accelerates lung damage via activation of the pro-inflammatory response and pulmonary fibrosis. J Microbiol Biotechnol 2020;30(3):427–38. https://doi.org/10.4014/jmb.1910.10055.

[16] Ma C, Wang L, Tao X, Zhang N, Yang Y, Tseng C-T, et al. Searching for an ideal vaccine candidate among different MERS coronavirus receptor-binding fragments—the importance of immunofocusing in subunit vaccine design. Vaccine 2014;32(46):6170–6. https://doi.org/10.1016/j.vaccine.2014.08.086.

[17] Lee JY, Bae S, Myoung J. Middle East respiratory syndrome coronavirus-encoded accessory proteins impair MDA5-and TBK1-mediated activation of NF-κB. J Microbiol Biotechnol 2019;28;29(8):1316–1323.. https://doi.org/10.4014/jmb.1908.08004.

[18] Weiskopf D, Angelo MA, Bangs DJ, Sidney J, Paul S, Peters B, et al. The human $CD8^+$ T cell responses induced by a live attenuated tetravalent dengue vaccine are directed against highly conserved epitopes. J Virol 2015;89(1):120–8. https://doi.org/10.1128/JVI.02129-14.

[19] Williamson JS, Stohlman SA. Effective clearance of mouse hepatitis virus from the central nervous system requires both $CD4^+$ and $CD8^+$ T cells. J Virol 1990;64(9):4589–92. https://doi.org/10.1128/jvi.64.9.4589-4592.1990.

[20] Harty JT, Tvinnereim AR, White DW. $CD8^+$ T cell effector mechanisms in resistance to infection. Annu Rev Immunol 2000;18(1):275–308. https://doi.org/10.1146/annurev.immunol.18.1.275.

[21] Betts MR, Brenchley JM, Price DA, De Rosa SC, Douek DC, Roederer M, et al. Sensitive and viable identification of antigen-specific $CD8^+$ T cells by a flow cytometric assay for degranulation. J Immunol Methods 2003;281(1-2):65–78. https://doi.org/10.1016/S0022-1759(03)00265-5.

[22] Appay V, Zaunders JJ, Papagno L, Sutton J, Jaramillo A, Waters A, et al. Characterization of $CD4^+$ CTLs ex vivo. J Immunol 2002;168(11):5954–8. https://doi.org/10.4049/jimmunol.168.11.5954.

[23] van Leeuwen EMM, Remmerswaal EBM, Vossen MTM, Rowshani AT, Wertheim-van Dillen PME, van Lier RAW, et al. Emergence of a $CD4^+$ $CD28^-$ granzyme $^B+$, cytomegalovirus-specific T cell subset after recovery of primary cytomegalovirus infection. J Immunol 2004;173(3):1834–41. https://doi.org/10.4049/jimmunol.173.3.1834.

[24] Takeuchi A, Saito T. CD4 CTL, a cytotoxic subset of $CD4^+$ T cells, their differentiation and function. Front Immunol 2017;8:194. https://doi.org/10.3389/fimmu.2017.00194.

[25] Pascal KE, Coleman CM, Mujica AO, Kamat V, Badithe A, Fairhurst J, et al. Pre- and postexposure efficacy of fully human antibodies against Spike protein in a novel humanized mouse model of MERS-CoV infection. Proc Natl Acad Sci USA 2015;112(28):8738–43. https://doi.org/10.1073/pnas.1510830112.

[26] Molaei S, Dadkhah M, Asghariazar V, Karami C, Safarzadeh E. The immune response and immune evasion characteristics in SARS-CoV, MERS-CoV, and SARS-CoV-2: Vaccine design strategies. Int Immunopharmacol 2021;92:107051. https://doi.org/10.1016/j.intimp.2020.107051.

[27] Ma C, Li Ye, Wang L, Zhao G, Tao X, Tseng C-T, et al. Intranasal vaccination with recombinant receptor-binding domain of MERS-CoV spike protein induces much stronger local mucosal immune responses than subcutaneous immunization: Implication for designing novel mucosal MERS vaccines. Vaccine 2014;32(18):2100–8. https://doi.org/10.1016/j.vaccine.2014.02.004.

[28] Chen Y, Rajashankar KR, Yang Y, Agnihothram SS, Liu C, Lin Y-L, et al. Crystal structure of the receptor-binding domain from newly emerged Middle East respiratory syndrome coronavirus. J Virol 2013;87(19):10777–83. https://doi.org/10.1128/JVI.01756-13.

[29] Lu G, Hu Y, Wang Q, Qi J, Gao F, Li Y, et al. Molecular basis of binding between novel human coronavirus MERS-CoV and its receptor CD26. Nature 2013;500 (7461):227–31. https://doi.org/10.1038/nature12328.

[30] Tang J, Zhang N, Tao X, Zhao G, Guo Y, Tseng C-T, et al. Optimization of antigen dose for a receptor-binding domain-based subunit vaccine against MERS coronavirus. Hum Vaccin Immunother 2015;11(5):1244–50. https://doi.org/10.1080/21645515.2015.1021527.

[31] Nassar M, Bakhrebah M, Meo S, Alsuabeyl M, Zaher WA. Middle East Respiratory Syndrome Coronavirus (MERS-CoV) infection: epidemiology, pathogenesis and clinical characteristics. Eur Rev Med Pharmacol Sci 2018;22:4956–61. https://doi.org/10.1016/j.jmii.2018.04.005.

[32] Lee S, Nguyen MT. Recent advances of vaccine adjuvants for infectious diseases. Immune Netw 2015;15:51–7. https://doi.org/10.4110/in.2015.15.2.51.

[33] Brandtzaeg P. Role of secretory antibodies in the defence against infections. Int J Med Microbiol 2003;293(1):3–15. https://doi.org/10.1078/1438-4221-00241.

[34] Marshall NB, Swain SL. Cytotoxic CD4 T cells in antiviral immunity. J Biomed Biotechnol 2011;2011:1–8. https://doi.org/10.1155/2011/954602.

[35] Brown DM, Lee S, Garcia-Hernandez MdlL, Swain SL. Multifunctional CD4 cells expressing gamma interferon and perforin mediate protection against lethal influenza virus infection. J Virol 2012;86(12):6792–803. https://doi.org/10.1128/JVI.07172-11.

[36] Lau SKP, Lau CCY, Chan K-H, Li CPY, Chen H, Jin D-Y, et al. Delayed induction of proinflammatory cytokines and suppression of innate antiviral response by the novel Middle East respiratory syndrome coronavirus: implications for pathogenesis and treatment. J Gen Virol 2013;94(12):2679–90. https://doi.org/10.1099/vir.0.055533-0.

[37] Dong Y, Dai T, Wei Y, Zhang L, Zheng M, Zhou F. A systematic review of SARS-CoV-2 vaccine candidates. Signal Transduct Target Ther 2020;5:1–14. https://doi.org/10.1038/s41392-020-00352-y.

[38] Rogers TF, Zhao F, Huang D, Beutler N, Burns A, He W-T, et al. Isolation of potent SARS-CoV-2 neutralizing antibodies and protection from disease in a small animal model. Science 2020;369(6506):956–63.

[39] Yasui F, Kai C, Kitabatake M, Inoue S, Yoneda M, Yokochi S, et al. Prior Immunization with severe acute respiratory syndrome (SARS)-associated coronavirus (SARS-CoV) nucleocapsid protein causes severe pneumonia in mice infected with SARS-CoV. J Immunol 2008;181(9):6337–48. https://doi.org/10.4049/jimmunol.181.9.6337.

[40] Kumar P, Chen K, Kolls JK. Th17 cell based vaccines in mucosal immunity. Curr Opin Immunol 2013;25(3):373–80. https://doi.org/10.1016/j.coi.2013.03.011.

[41] Riera-Borrull M, Cuevas VD, Alonso B, Vega MA, Joven J, Izquierdo E, et al. Palmitate conditions macrophages for enhanced responses toward inflammatory stimuli via JNK activation. J Immunol 2017;199(11):3858–69. https://doi.org/10.4049/jimmunol.1700845.